International Journal of

Applied Ceramic TECHNOLOGY

Ceramic Product Development and Commercialization

Nondestructive Evaluation (NDE) for Characterizing Oxidation Damage in Cracked Reinforced Carbon–Carbon

Don J. Roth* and Nathan S. Jacobson

NASA Glenn Research Center, Cleveland, Ohio 44135

Richard W. Rauser

University of Toledo, Toledo, Ohio 43606

Russell A. Wincheski

NASA Langley Research Center, Hampton, Virginia 23681

James L. Walker

NASA Marshall Space Flight Center, Huntsville, Alabama 35812

Laura A. Cosgriff

Cleveland State University, Cleveland, Ohio 44115

In this study, coated reinforced carbon–carbon (RCC) samples of similar structure and composition as that from the NASA space shuttle orbiter's thermal protection system were fabricated with slots in their coating simulating craze cracks. These specimens were used to study oxidation damage detection and characterization using nondestructive evaluation (NDE) methods. These specimens were heat treated in air at 1143°C and 1200°C to create cavities in the carbon substrate underneath the coating as oxygen

*donald.j.roth@nasa.gov

reacted with the carbon and resulted in its consumption. The cavities varied in diameter from approximately 1 to 3 mm. Single-sided NDE methods were used because they might be practical for on-wing inspection, while X-ray micro-computed tomography (CT) was used to measure cavity sizes in order to validate oxidation models under development for carbon–carbon materials. An RCC sample having a naturally cracked coating and subsequent oxidation damage was also studied with X-ray micro-CT. This effort is a follow-on study to one that characterized NDE methods for assessing oxidation damage in an RCC sample with drilled holes in the coating.

Introduction

Reinforced carbon–carbon (RCC) with a silicon carbide (SiC) coating for oxidation resistance is used on the NASA Space Shuttle Orbiter's wing leading edge, nose cap, and arrowhead attachment point to the external tank for thermal protection during reentry. The high strength and light weight of RCC make it an ideal aerospace material; however, oxidation is a major concern. Oxidation damage to RCC can occur if the SiC coating is itself damaged but still intact such that hot gases have access to the carbon beneath the coating.[1] In such cases, it is critical to evaluate the extent of the oxidation damage underneath the intact SiC coating. Even small breaches in the RCC coating system have recently been identified as potentially serious. In a prior study, small breaches in the coating of an RCC sample were created by drilling holes followed by oxidation of the sample and subsequent nondestructive evaluation (NDE) to characterize oxidation damage.[2] In that study, RCC samples were oxidized to create approximately hemi spherical holes underneath the SiC coating and subsequently inspected using various NDE methods. In the current study, small breaches were created by machining slots of various widths to simulate cracks of various sizes in the coating, and NDE was again subsequently used to characterize the oxidation damage.

The NDE techniques used in this study included state-of-the-art backscatter X-ray (BSX), ultrasonic-guided waves, eddy current (EC), and thermographic methods. All of these methods are single-sided techniques thereby lending themselves to practical inspections of components only accessible from
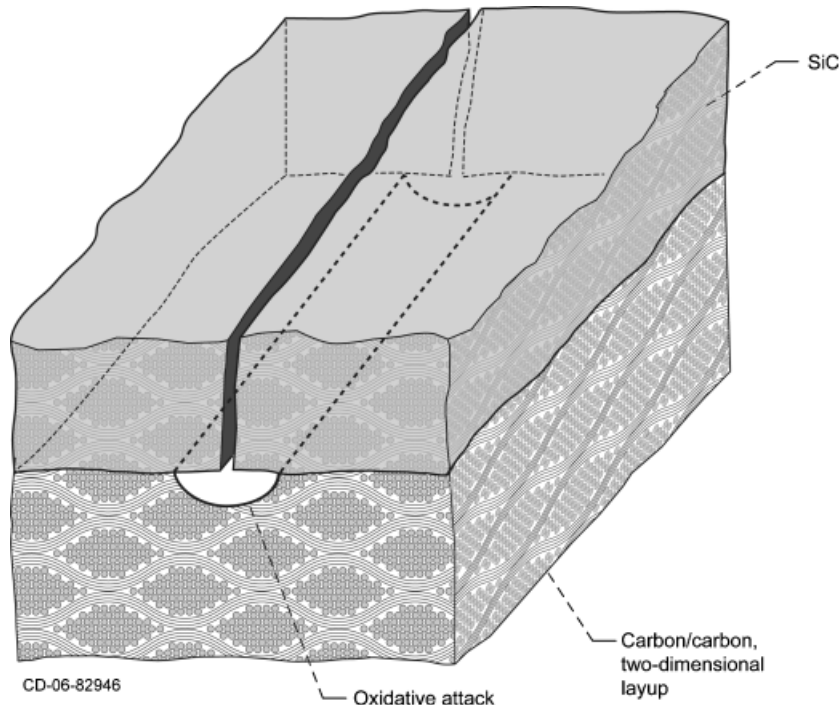

CD-06-82946

Fig. 1.   Schematic of silicon carbide (SiC)-protected carbon/carbon used in this study. Reprinted with permission from Elsevier.
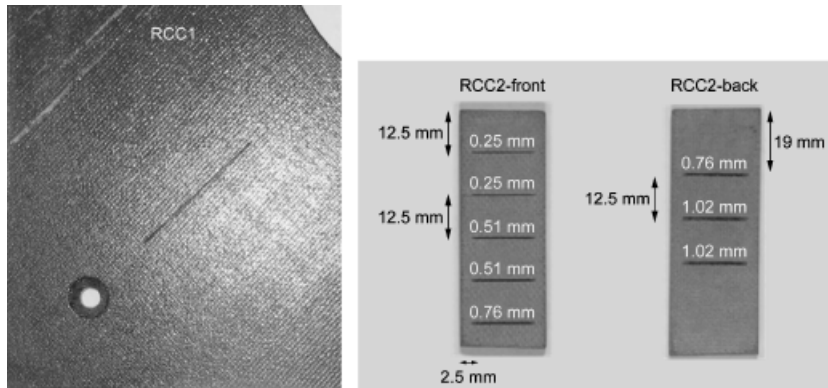
Fig. 2.   Photographs of machined reinforced carbon–carbon (RCC) samples with machined slots. Nominal widths of slots are shown above the slot and spacing between slots and from edges is also shown.

one side. Samples were also inspected with X-ray micro-computed tomography (CT) to evaluate the true dimensions and morphology of the holes, as well as natural crack formations.[3] The controlled oxidation damage provides standards for investigating the effectiveness of various NDE techniques for detecting and sizing oxidation damage in this material. NASA Glenn Research Center led this investigation that had some of the top NDE specialists/facilities from NASA Glenn, NASA Langley, and NASA Marshall inspect these samples with the various NDE methods.

Experimental Procedure

RCC Material

Figure 1 is a schematic of RCC with a SiC conversion coating. Briefly, this material is made with a two-dimensional layup of carbon–carbon fabric with repeated applications of a liquid carbon precursor to fill voids. An oxidation protection system is based on a SiC conversion coating. Because of the difference in coefficient of thermal expansion of the SiC coating and carbon/carbon substrate, the SiC coating shrinks more than the underlying carbon/carbon on cooldown from the coating application temperature. This leads to vertical cracks in the coating, and these cracks are pathways for oxygen to reach the carbon/carbon substrate. Actual RCC used on the Space Shuttle Orbiter is infiltrated with tetraethyl orthosilicate (TEOS), which decomposes on a mild heat treatment to silica. Then the RCC sur-

faces are painted with a sodium silicate glass, which melts and seals cracks on reentry. All the samples used in this study had the TEOS treatment. In addition, one of the samples studied had the sodium silicate glass. The samples were all approximately 5 mm thick.

The sample with SiC plus glass coating (RCC1) was a flat plate with an approximately 1 mm thick SiC plus glass coating and coated on all sides. The plate had an artificial craze crack of linear geometry made with a diamond blade (Keen Kut Products, Hayward, CA) of 0.25 mm thickness. This plate was used for ultrasonic studies. The slot was cut to the SiC plus glass coating/carbon–carbon interface on one side of the sample.

The samples with only the SiC coating had an approximately 1-mm-thick coating and were coated on all sides. Of these, one was a plate. The plate (RCC2) had machined slots made with diamond blades of 0.25, 0.51, 0.76, and 1.02 mm thicknesses. These slots were cut to the SiC/carbon–carbon interface on both sides of the plate ample. These slotted specimens are shown in Fig. 2.

Other SiC-only coated samples included several flat 1.91 cm diameter and 1.52-cm-thick disks.[3] Some of these had slots machined in them; others were used in their as-fabricated form with the naturally occurring craze cracks acting as paths for oxidation. Polishing $\sim 300\,\mu m$ of SiC off the surface showed the cellular crack pattern as shown in Fig. 3a together with a "skeleton" trace of the cracks in Fig. 3b.

Controlled laboratory oxidation exposures were performed as follows: (a) Plates and disks with machined slots: 0.5 h at 1200°C in static laboratory air; (b) Disk with craze cracks only: 2.5 h in bottle flowing air at
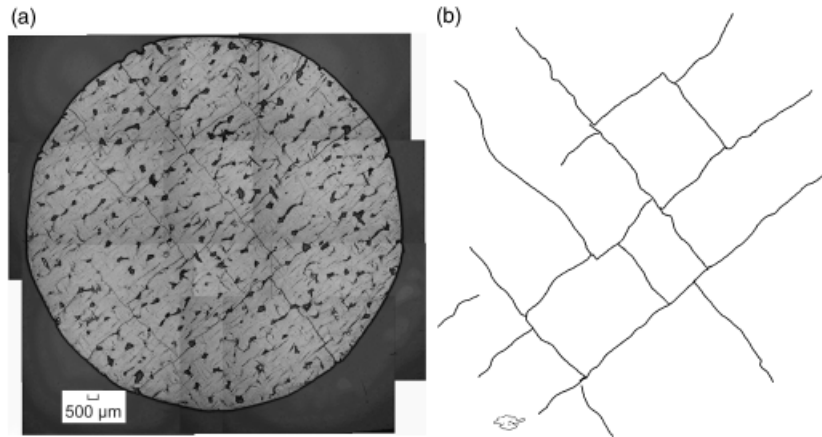
Fig. 3. (a) Reinforced carbon–carbon disk with craze crack pattern on the surface. (b) "Skeleton" trace of crack pattern. Reprinted with permission from Elsevier.

1143°C. The carbon/carbon substrate below the machined slot oxidized to form an approximate hemispherical void (Fig. 4). This uniform attack pattern indicates diffusion control; and Jacobson *et al.*[3] describes an oxidation model for given slot and crack breaches in the coating. The resulting size of the void would be expected to increase with increasing slot width. Depth and diameter of voids in this study tended to be on the order of 1–3 mm. This controlled oxidation damage provides standards for investigating the effectiveness of various NDE techniques for detecting and sizing this type of oxidation damage in this material.

NDE

Various single-sided state-of-the-art NDE methods were used to characterize the RCC samples before (baseline condition), and after, oxidation. These methods included BSX, EC, thermography, and guided wave ultrasonics. X-ray CT was used to size oxidation damage and cracking, and develop three-dimensional volumetric visualizations. Dugan and colleagues[4–8] provide basic principles for the various methods, and experimental parameters for the methods are given here. Specialized image processing was used as needed to highlight indications from the NDE methods using software developed at NASA and available in the public domain.[9] The software processing generally consisted of the following operations (in the following sequence): image crop, contrast expansion, outlier (bad value) removal, and wavelet denoise. If the processing was applied, it was applied identically to the images of pre- and postoxidation NDE images.
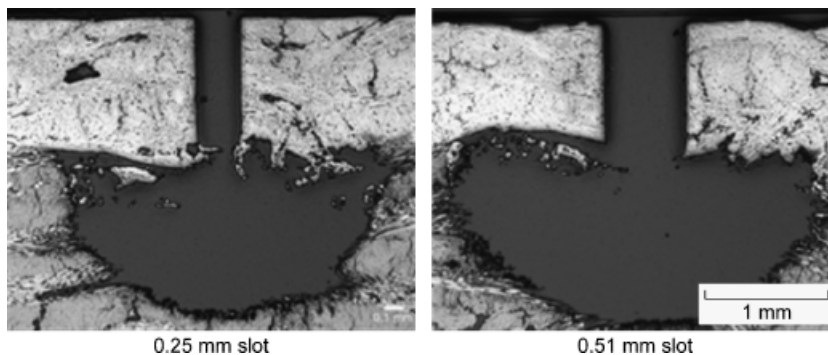

0.25 mm slot   0.51 mm slot

Fig. 4. Cross-sections of cavity resulting from oxidation treatment for the slotted disks with an oxidation treatment for 0.5 h in 1200°C static laboratory air.

BSX: A scanning BSX system was used to image the RCC samples.[4] Several parameter settings were used to determine optimized conditions but for the purposes of comparing pre- and postoxidation images, the following settings were used in those cases. The settings were aperture of 2 mm, voltage of 55 kV, current of 11.6 mA, focal spot size of 1 mm, finned collimator angle of 90° and exposure time per scan position of 0.2 s. The scan parameters included scan (X) and step (Y) increments of 0.5 mm and scan velocity of 2.5 mm/s. Scans were performed from both sides of the RCC2 sample.

EC: Scanning EC inspection of the RCC sample was accomplished using a high-frequency EC surface probe connected through a spring loaded z-axis gimbal to an x/y scanning system. In the present work a probe drive frequency of 5 MHz and scan spacing of 0.025 in. were used. Calibration of the system is performed using an uncoated RCC test article of nominally matching conductivity to the part under test. The probe response is rotated such that lift-off is in the horizontal direction. Nonconductive plastic shims are then used to measure the nominal SiC coating thickness (lift-off) and lift-off sensitivity. Oxidation damage under the SiC coating is measured as a localized increase in lift-off due to the increased spacing between the sensor and the conducting carbon–carbon substrate in the oxidized areas. Scans were performed from both sides of the sample. The differences in conductivity/lift-off values are displayed in various shades of gray in the c-scan image. The system used in this study minimized edge effects as compared with the one used in Roth *et al.*[2]

Thermography: A pulsed full-field thermographic NDE method utilizing flash lamps and a high-speed camera was used to obtain images of the RCC sample.[6] The system consists of two high-energy xenon flash lamps, each capable of producing a 1.8 kJ flash with a 5 ms duration. The flash lamps were placed at locations that provide a relatively uniform distribution of heat across the surface of the specimen. The transient thermal response of the specimen after flashing was captured using high-speed infrared camera. The camera used in the study is a 640 by 512 InSb focal plane array type with a 14-bit dynamic range. The camera operates in the 3–5 μm wavelength range and is capable of capturing thermal data at rates of 30 Hz for the full-array size. For this study, a 320 by 256 portion of the full array was utilized in order to increase the frame rate to approximately 60 Hz. Flash initiation, data collection, storage,

and processing were all performed using software on the acquisition computer. Experimental data were collected using the following procedure. The specimen was placed in front of the infrared (IR) camera at a distance that allowed the sample to fill most of the active focal plane and then focused. Flash lamps were set at a distance of approximately 300 mm. from the sample at an angle of 45°. Along with the images captured after the flash, six preflash images were collected. Instantaneous and derivative images (from relative temperature versus time) were obtained, and the operator normally selected the best images for analysis using a subjective process of selecting frames of maximum contrast. Thermography was performed from both sides of the sample. The differences in surface temperature are displayed in various shades of gray in the image.

Ultrasonic-Guided Waves: An ultrasonic-guided wave measurement system[7] was used to determine whether total ultrasonic energy (M_0) of the time domain guided waveform was altered by the addition of the slot (artificial crack) and oxidation of the RCC1 sample containing the single slot. M_0 is calculated from the area under the curve of the power spectral density $S(f)$ of the time domain waveform according to

$$M_0 = \int_{f_{\text{low}}}^{f_{\text{high}}} S(f)df \qquad (1)$$

where f_{low} and f_{high} are the lower and upper frequency (f) bounds of the integration range, respectively. Total energy is a physically understandable parameter that would likely be altered due to ultrasonic scattering both by the addition of the slot into the ultrasonic path and after further alterations of the slot due to oxidation and glass filling. Broadband ultrasonic transducers were used with center frequencies of approximately 1 MHz (both sender and receiver were of the same frequency). Multiple mode excitation is likely due to the use of broadband transducers and the existence of multiple plate wave modes is confirmed by the complicated nature of the signal.[7] Ultrasound was coupled to the material via elastic coupling pads. The distance between sending and receiving transducers was 2.5 cm. For the baseline (before slotting) condition of the RCC1 sample (Fig. 2), the transducers were positioned so that they would straddle the future position of the slot, and then after slotting, they were positioned identically such that they straddled the slot.

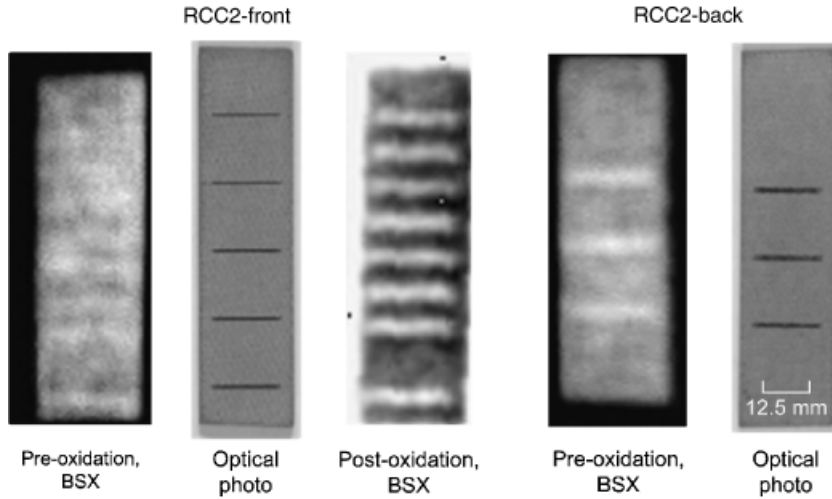Analog-to-digital sampling rate for the ultrasonic testing was 10 MHz. A measurement was made (contact

Fig. 5. Backscatter X-ray (BSX) results.

load $= 3.63+0.23$ kg [8+0.5 lb]), the sender–receiver pair was lifted, moved to the next location, lowered to be in contact with the sample, and another measurement made. Twenty measurements were obtained (2 columns $\times$ 10 rows) with measurements separated by 1 mm, and mean and standard deviation of (M_0) was calculated. The identical pattern of measurements was made before slotting, after slotting, after oxidation, and after removing glass sealant from the crack followed by a second oxidation. Additionally, the final scan was done five times to measure reproducibility of the technique. In a future investigation, the effect of the slot and oxidation on other ultrasonic parameters that can be derived from broadband ultrasonic-guided wave signals will be considered.[7–9]

X-Ray CT: X-ray CT was used to provide additional images of the oxidation damage and study oxidation in the naturally cracked RCC sample, without destructive sectioning.[8] This SmartScan Model 100 (CITA Systems, Pueblo, CO) system utilizes a Feinfocus FXE–160 (COMET AG, Flamatt, Switzerland) microfocus X-ray source to produce very high-resolution imaging of samples, approaching 0.025 mm, in the CT mode of operation. The major hardware components of this system included the X-ray source, an area detector system, a five-axis object positioning subassembly, and a lead-lined radiation cabinet. A dual-processor computer system controlled the data acquisition and image processing. The slice plane thickness was 0.120 mm per slice for
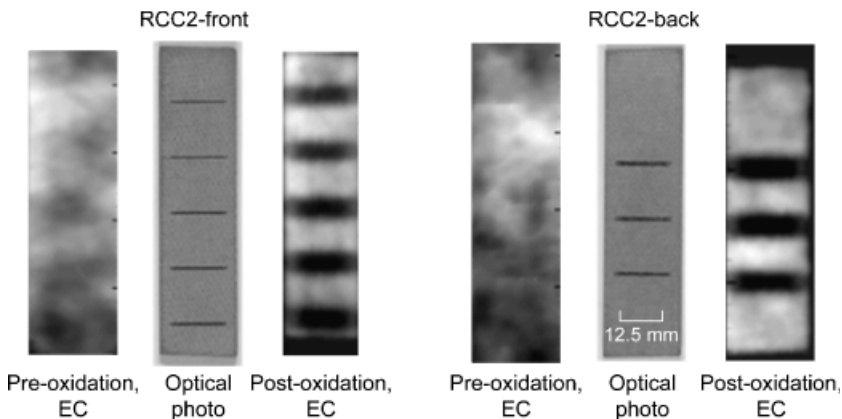

Fig. 6. Eddy current (EC) results.

RCC2-front

RCC2-back

Pre-oxidation, thermography | Optical photo | Post-oxidation, thermography

12.5 mm

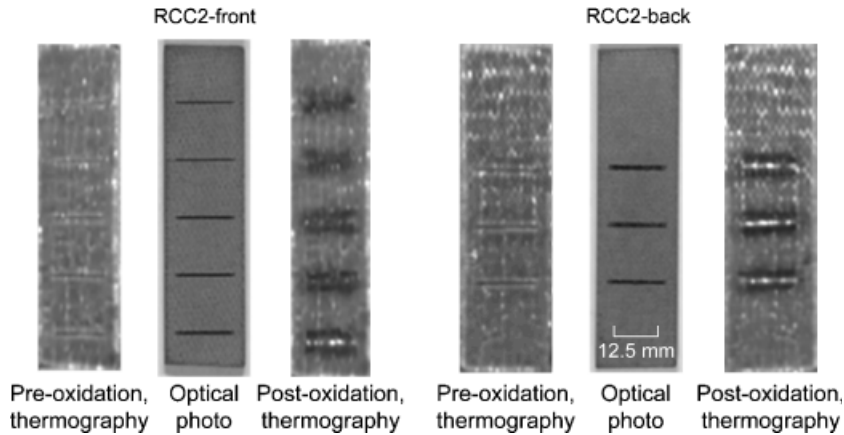Pre-oxidation, thermography | Optical photo | Post-oxidation, thermography

Fig. 7. Thermographic (derivative) image results. Preoxidation images are frames at 0.18 s in the temperature versus time cooldown stream of frames. Postoxidation images are frames at 0.164 s in the temperature versus time cooldown stream of frames.
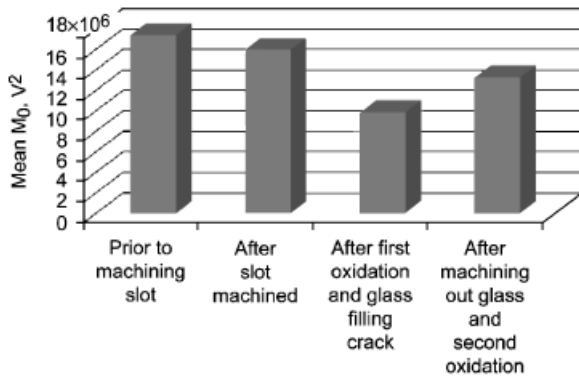

Fig. 8. Ultrasonic guided wave (mean total energy M_0) results on sample reinforced carbon–carbon1 (Fig. 2). Measurement variability is about 2% based on repeated trials.

these samples. Putting together slices electronically gave a three-dimensional view of oxidation damage. The sample was placed on a micropositioner between the source and detector, which allowed positioning and rotation to obtain the slice images. The differences in X-ray density are displayed in various shades of gray.

Results and Discussion

Figures 5–9 show NDE results including images of the samples before and after oxidation. Figure 5 shows BSX results. Before oxidation, indications of the slots were difficult to discriminate when the X-ray source faced the RCC2 sample face with five slots (front) except for the bottommost slot which was approximately 0.76 mm wide (the widest of the five slots on that face). When the X-ray source faced the sample face having with three slots (back), those three slots could be discriminated fairly easily due to their large width (0.76 and 1.02 mm) before oxidation. Postoxidation, all eight slots were easily discriminated with the X-ray source facing the front face indicating the extensive depth of
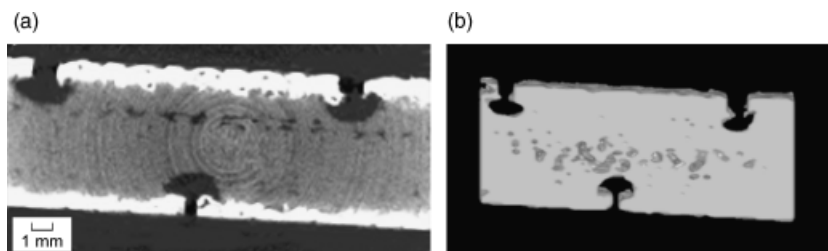

Fig. 9. (a) Contrast-enhanced X-ray computer tomography (CT) slice of portion of reinforced carbon–carbon2 sample. Ring pattern is an artifact of the CT processing. (b) Solid three-dimensional visualization constructed from CT slices.
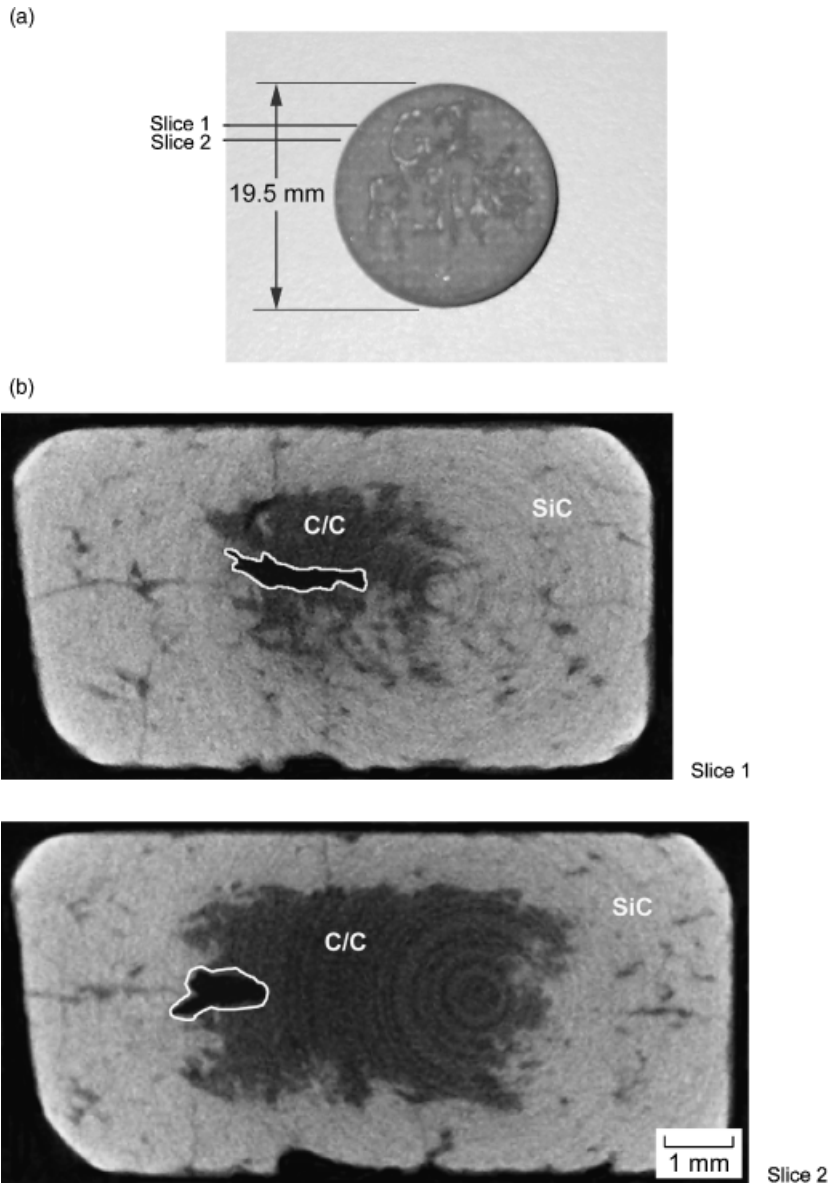
Fig. 10.   X-ray computer tomography (CT) of silicon carbide (SiC)-coated reinforced carbon–carbon oxidized for 2.5 h in air at 1143°C. (a) Location of CT slices. (b) Two CT slices. Reprinted with permission from Elsevier.

damage created by the oxidation. A postoxidation BSX image with X-ray source facing the back face is not shown (nor necessary) because all slots were showed with X-ray source facing the front face postoxidation.

Figure 6 shows EC results. Slots were impossible to discriminate before oxidation but were easily discriminated after oxidation. Eddy current required scanning

from both sides to allow visualization of each face's slots. Qualitatively, the larger slots appeared to give more pronounced indications.

Figure 7 shows thermography (derivative image) results. Slots were modestly discriminated before oxidation and were easily discriminated after oxidation. The heat source and thermography camera were facing

the slots in order for oxidation damage detection to occur.

Figure 8 shows ultrasonic-guided wave (mean total energy M_0) results for RCC1 with the single machined slot. The guided wave technique is extremely sensitive to surface condition and the optical appearance of the surface appeared the same both before (baseline) and after oxidation. Controlled, identical force was present on the ultrasonic transducers for the ultrasonic measurements before and after oxidation. As compared with mean M_0 of the time domain wave for the baseline condition (before machining slot), mean M_0 had decreased after machining, after first oxidation, and after machining out glass in the slot and performing a second oxidation. However, the decrease was not monotonic for these steps. The general decrease in M_0 after slotting and subsequent oxidation treatments is indicative of the slot structure scattering the ultrasound such that less ultrasonic energy reaches than receiving transducer as compared with the baseline (no slot) condition. Note that the repeatability of the measurement method was good. The five scans that were repeated after the final step show variability of mean M_0 to be about 2%, which is significantly <8% decrease in M_0 noted from baseline to after slot machined condition. This variability is dependent upon surface condition and measurement load remaining very similar.

Figure 9a shows an X-ray CT slice of a portion of the RCC2 sample showing the 0.25, 0.51, and 1.02 mm slots and the hemi spherical oxidation damage beneath the SiC coating and slots. CT has been used to size the hemispherical regions in order to help validate and/or show deviations from the oxidation model discussed in.[1–3] The size of the voids showed by CT was on the order of 1–3 mm for depth and diameter, depending on the slot width. CT sizing was generally within 5–10% of actual values from destructive sectioning of several of the sample portions. X-ray CT allows the ability to sweep through various cross-sections and find the maximum diameter nondestructively and thus can result in a more accurate value for void diameter than destructive sectioning. Three-dimensional visualizations and animations composed of 11 consecutive CT slices were prepared on different sections of test samples, with one solid visualization shown in Fig. 9b. These help show additional morphological features of the damage due to the three-dimensional nature.

The high resolution of the X-ray CT technique makes it suitable for probing the oxidation damage below craze cracks, as this damage tends to be smaller and much more irregular than the damage below the machined slots. Figure 10 shows two X-ray CT slices for a naturally cracked RCC sample with the outlined area indicating the oxidation damage below the natural crack paths. The oxidation cavity shapes are highly irregular, as expected from the varying coating thickness and irregular nature of the cracks.[3] Figure 11 shows a translucent three-dimensional visualization constructed from 11 consecutive CT slices of this sample.

Summary

In this study, RCC samples having slots in their coating machined to the depth of the SiC coating, underwent oxidation treatments to create void-like damage in the carbon–carbon substrate underneath the coating. The size of the voids showed by X-ray micro-CT was on the order of 1–3 mm for depth and diameter, depending on the slot width. State-of-the-art single-sided NDE methods, practical where access to only one side of the structure is available such as for on-wing inspections, were used to detect the damage. These methods included BSX, EC, thermography, and ultrasonic guided waves. All of the methods were successful at detecting the oxidation damage, whereas only thermography unambiguously showed the slots before oxidation. The higher resolution of the CT technique made it suitable to quantitatively assess oxidization damage both below machined slots and craze cracks. Further this technique showed the patterns of oxidation attack, which tended to be smaller and much more irregular below the craze cracks than under machined slots. Changes in ultrasonic-guided wave total energy show this parameter is sensitive to structural changes in RCC.
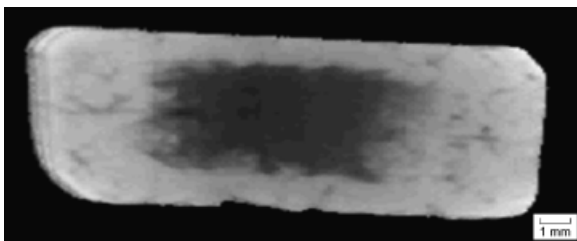

Fig. 11.   Translucent three-dimensional visualization constructed from X-ray computer tomography slices of sample shown in Fig. 10.

References

1. N. S. Jacobson, T. A. Leonhardt, D. M. Curry, and R. A. Rapp, "Oxidative Attack of Carbon/Carbon Substrates Through Coating Pinholes," *Carbon*, 37 411–419 (1999).
2. D. J. Roth, N. S. Jacobson, J. N. Gray, L. M. Cosgriff, J. R. Bodis, R. A. Wincheski, R. W. Rauser, E. A. Burns, and M. S. McQuater, "N*DE* for Characterizing Oxidation Damage in Reinforced Carbon–Carbon Used on the NASA Space Shuttle Thermal Protection System," *Ceram. Eng. Sci. Proc.*, 26 [2] 133–141 (2006).
3. N. S. Jacobson, D. J. Roth, R. W. Rauser, J. D. Cawley, and D. M. Curry, "Oxidation Through Coating Cracks of SiC-Protected Carbon/Carbon," *Surf. Coat. Tech.*, 203 372–383 (2008).
4. E. Dugan, A. Jacobs, D. Shedlock, and D. Ekdahl "Detection of Defects in Foam Thermal Insulation Using Lateral Migration Backscatter X-ray Radiography," *Proceedings of SPIE 49th Annual Meeting, Symposium on Optical Science and Technology, Penetrating Radiation Systems and Applications VI*, Vol. 5541, Denver, August, 2004.
5. B. A. Wincheski and J. W. Simpson "Application of Eddy Current Techniques for Orbiter Reinforced Carbon–Carbon Structural Health Monitoring," Contract #23-376-70-30-05, 2005.
6. S. M. Shepard, J. R. Lhota, B. A. Rubadeux, and T. Ahmed "Onward and inward: Extending the limits of thermographic NDE," *Proceedings of the SPIE Thermosense XXII*, Vol. 4020, 2000, p. 194.
7. D. J. Roth, L. M. Cosgriff, M. J. Verilli, and R. T. Bhatt, "Microstructural and Discontinuity Characterization in Ceramic Composites Using an Ultrasonic Guided Wave Scan System," *Mater Eval.* 62 [9] 948–953 (2004).
8. R. N. Yancey, G. Y. Baaklini, and S. J. Klima. "NDE of Advanced Turbine Engine Components and Materials by Computed Tomography," *ASME, International Gas Turbine and Aeroengine Congress and Exposition*, 36th, Orlando, FL, June 3–6, 1991.
9. D. J. Roth, R. E. Martin, J. P. Seebo, L. B. Trinh, J. L. Walker, and W. P. Winfree "A Software Platform for Post-Processing Waveform-Based NDE," *SAMPE Proceedings and Presentation*, June 2007, Baltimore, MD.